Aerosol Chamber Study of Optical Constants and N_2O_5 Uptake on Supercooled $H_2SO_4/H_2O/HNO_3$ Solution Droplets at Polar Stratospheric Cloud Temperatures

Robert Wagner,* Karl-Heinz Naumann, Alexander Mangold,† Ottmar Möhler, Harald Saathoff, and Ulrich Schurath

Forschungszentrum Karlsruhe, Institute of Meteorology and Climate Research (IMK-AAF), Karlsruhe, Germany

Received: March 15, 2005; In Final Form: July 15, 2005

The mechanism of the formation of supercooled ternary $H_2SO_4/H_2O/HNO_3$ solution (STS) droplets in the polar winter stratosphere, i.e., the uptake of nitric acid and water onto background sulfate aerosols at $T <$ 195 K, was successfully mimicked during a simulation experiment at the large coolable aerosol chamber AIDA of Forschungszentrum Karlsruhe. Supercooled sulfuric acid droplets, acting as background aerosol, were added to the cooled AIDA vessel at $T = 193.6$ K, followed by the addition of ozone and nitrogen dioxide. N_2O_5, the product of the gas phase reaction between O_3 and NO_2, was then hydrolyzed in the liquid phase with an uptake coefficient $\gamma(N_2O_5)$. From this experiment, a series of FTIR extinction spectra of STS droplets was obtained, covering a broad range of different STS compositions. This infrared spectra sequence was used for a quantitative test of the accuracy of published infrared optical constants for STS aerosols, needed, for example, as input in remote sensing applications. The present findings indicate that the implementation of a mixing rule approach, i.e., calculating the refractive indices of ternary $H_2SO_4/H_2O/HNO_3$ solution droplets based on accurate reference data sets for the two binary H_2SO_4/H_2O and HNO_3/H_2O systems, is justified. Additional model calculations revealed that the uptake coefficient $\gamma(N_2O_5)$ on STS aerosols strongly decreases with increasing nitrate concentration in the particles, demonstrating that this so-called nitrate effect, already well-established from uptake experiments conducted at room temperature, is also dominant at stratospheric temperatures.

Introduction

Supercooled ternary $H_2SO_4/H_2O/HNO_3$ solution (STS) droplets form at temperatures <195 K during the polar night when nitric acid and water condense onto background sulfate aerosols. With decreasing temperature, the composition of the STS droplets may vary from almost pure sulfuric acid to almost pure nitric acid solution droplets, containing only a minor fraction of H_2SO_4 (about 5 wt % at temperatures close to the ice frost point).[1] Important experimental techniques to directly measure or to retrieve the STS composition include in situ aerosol composition mass spectrometry[2,3] as well as analysis of broadband mid-IR spectra recorded by remote sensing instruments.[4,5] In the latter case, the accuracy of the retrieved aerosol composition crucially depends on the quality of the employed low-temperature indices of refraction. As highlighted in a recent discussion of the complex indices of refraction contained in HITRAN,[6,7] significant differences still exist between individual laboratory data sets. In recent experiments, conducted in the large coolable aerosol chamber AIDA of Forschungszentrum Karlsruhe, we have quantitatively tested the accuracy of different laboratory data sets of refractive indices for binary H_2SO_4/H_2O and HNO_3/H_2O aerosols by comparing directly measured aerosol parameters (i.e., composition and mass concentration) with those retrieved from the analysis of FTIR extinction spectra.[8] We found close agreement between retrieved and independently measured aerosol parameters when using the Niedziela et al.[9] data set for the H_2SO_4/H_2O system and the Norman et al.[10] data set for the HNO_3/H_2O system. On the contrary, presumably due to procedural errors in extracting the refractive indices from thin film reference spectra, the Biermann et al.[11] data sets for the two binary systems failed to accurately reproduce our measured aerosol extinction spectra.

In the present paper, we will extend our study to the refractive indices of ternary $H_2SO_4/H_2O/HNO_3$ solution droplets. Biermann et al.[11] have proposed a mixing rule to calculate the imaginary part (k) of the complex refractive index for the ternary solutions as a linear combination of the k values of the two binary data sets. This approach has already been implemented in several retrieval algorithms in remote sensing applications.[12,13] However, there is still a need for an independent study to assess the accuracy by which FTIR extinction spectra of STS aerosols can be analyzed in terms of aerosol composition and mass concentration on the basis of this mixing rule. McPheat et al.[14] have observed large spectral differences between a measured STS droplet extinction spectrum and a Mie calculation using the Biermann et al.[11] mixing rule in the 750−1300 cm^{-1} spectral region. However, this must not be a result of a deficiency of the mixing rule but may be fully explained by the poor quality of the Biermann et al.[11] binary data sets, which were employed in the mixing rule calculation. Hence, in view of the results of our previous study, we recommend to use the binary data sets of Niedziela et al.[9] and Norman et al.[10] in the mixing rule approach. This was already tested by Norman et al.[15] when comparing the refractive index values calculated using the mixing rule with directly measured refractive index data for six discrete STS compositions (see Figures 14 and 15 in their publication). In view of the simplicity of the mixing rule, which,

* Corresponding author. E-mail: Robert.Wagner@imk.fzk.de.
† Forschungszentrum Jülich, Institute of Chemistry and Dynamics of the Geosphere I (ICG I): Stratosphere, Jülich, Germany.

10.1021/jp0513364 CCC: $30.25
Published on Web 08/19/2005

e.g., neglects chemical interaction between the nitrate and sulfate components in the mixture, the agreement between the directly measured and calculated data sets was quite satisfactory.

In our present study, as a further comprehensive test of the mixing rule approach, we have measured low-temperature FTIR spectra of supercooled ternary $H_2SO_4/H_2O/HNO_3$ aerosols for an extended range of different aerosol compositions. This was done in one single experiment by injecting supercooled H_2SO_4/H_2O droplets (acting as background aerosol) into the AIDA chamber, followed by the addition of ozone and nitrogen dioxide. Gas phase reaction between O_3 and NO_2 yielded N_2O_5, which then hydrolyzed in the liquid phase, forming ternary $H_2SO_4/H_2O/HNO_3$ solution droplets with gradually increasing nitric acid concentration. As in our former study, we applied a fitting algorithm based on Mie theory to retrieve composition and mass concentration of the STS droplets. These data were then compared to those independently measured using complementary techniques (filter analysis, gas phase and total water measurements, and application of the thermodynamic equilibrium model by Carslaw et al.[16]).

In addition to the quantitative test of optical constants for ternary $H_2SO_4/H_2O/HNO_3$ solution droplets, the present experiment was used to determine the uptake coefficient $\gamma(N_2O_5)$ on liquid sulfuric acid and STS droplets at stratospheric temperatures. The N_2O_5 hydrolysis on H_2SO_4/H_2O has already been investigated in a number of laboratory studies, summarized in the IUPAC Subcommittee on Gas Kinetic Data Evaluation − Data Sheet R1 (http://www.iupac-kinetic.ch.cam.ac.uk/). Most measurements indicate that the uptake coefficient is only weakly dependent on the H_2SO_4 concentration and quite insensitive to changes in temperature. It was also concluded in the summary of the IUPAC data sheet that ternary $H_2SO_4/H_2O/HNO_3$ solutions behave identically to the binary H_2SO_4/H_2O system. However, the results concerning the effect of increasing nitric acid content on $\gamma(N_2O_5)$ are still contradictory. A so-called nitrate effect, i.e., a reduction of $\gamma(N_2O_5)$ on liquid aerosols with increasing nitrate concentration, has been clearly identified in recent measurements conducted at ambient temperatures in the aerosol chamber at Forschungszentrum Jülich.[17] As the ionic equilibrium $N_2O_5(aq) \rightleftarrows NO_2^+(aq) + NO_3^-(aq)$ is supposed to be the rate-determining step in the N_2O_5 hydrolysis,[18] an increasing nitrate concentration would shift the equilibrium reaction toward undissociated N_2O_5, thus suppressing the N_2O_5 reactivity. However, measurements performed by Hanson[19] at 201−230 K showed no clear evidence of a $\gamma(N_2O_5)$ reduction when going from a binary 60 wt % H_2SO_4 to a ternary 45 wt % H_2SO_4 + 15 wt % HNO_3 aqueous solution. The observed 15−20% decrease in $\gamma(N_2O_5)$ was comparable to the estimated uncertainty range of the data. On the contrary, Zhang et al.,[20] who worked at temperatures between 195 and 227 K, already observed a 60% decrease in $\gamma(N_2O_5)$ between solutions containing 53 wt % H_2SO_4 and 40 wt % H_2SO_4 + 10 wt % HNO_3. A reduction of $\gamma(N_2O_5)$ by a factor of 5 occurred when further increasing the nitric acid content to 40 wt %.

To clarify the magnitude of the nitrate effect in the heterogeneous uptake of N_2O_5 on STS aerosols, the present AIDA experiment is ideally suited due to the fact that the nitric acid concentration of the in situ produced STS droplets gradually increases with time. A model calculation for the determination of $\gamma(N_2O_5)$, which uses the uptake coefficient as adjustable parameter, will clearly show whether a constant $\gamma(N_2O_5)$ value is appropriate to fit the experimental data (meaning that no nitrate effect could be detected) or whether $\gamma(N_2O_5)$ has to be significantly reduced in course of time (i.e., increasing nitrate concentration) to fit the measured N_2O_5 uptake.

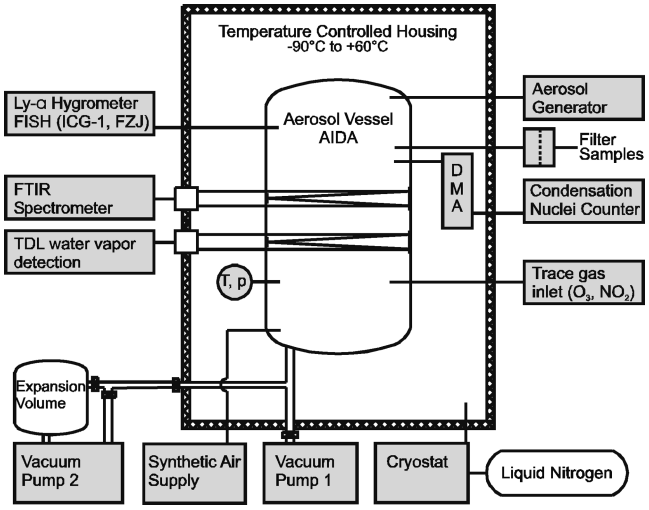

Figure 1. Schematic cross section of the AIDA facility showing the scientific instrumentation used in this study. The cylindrical aluminum vessel, volume 84 m^3, is mounted inside a large isolating housing. For the present experiment, the interior of this cold box, and thus the AIDA vessel, was cooled to a temperature of 193.6 K (see Möhler et al.[21] for technical details concerning the cooling system). The smaller aerosol vessel, located next to the main chamber, may be used as additional expansion volume in AIDA ice nucleation experiments.[21]

Methods

AIDA Setup. A detailed technical description of the low-temperature AIDA aerosol chamber facility of Forschungszentrum Karlsruhe can be found in our earlier publications.[8,21,22] Here, we will briefly review the major scientific instrumentation used for the experiment discussed in this paper, also shown as schematic cross section in Figure 1.

FTIR Spectroscopy. FTIR extinction spectra of the investigated species (i.e., absorption and scattering of the supercooled solution droplets plus absorbance of the reactive trace gases) were measured in situ with a White-type multiple reflection cell, mounted horizontally at 3.5 m height in the AIDA vessel and allowing optical path lengths of up to 250 m. Spectra were recorded with a FTIR spectrometer (Bruker, type IFS 66v) from 6000 to 800 cm^{-1} at a resolution of 4 wavenumbers. The quantitative analysis of the FTIR spectra (retrieval of aerosol parameters and trace gas mixing ratios) will be described in a separate section below.

Humidity Measurements. As in our previous study, we used the fast in situ Lyman-α hygrometer FISH of Forschungszentrum Jülich for water measurements.[23] Because the instrument was operated in an ex situ mode by sampling AIDA air through a heated inlet tube ($T > 293$ K), the total water mixing ratio (i.e., the sum of interstitial water vapor and evaporated particle water) was recorded. In addition, the interstitial water vapor pressure was directly measured in situ by tunable diode laser (TDL) absorption spectroscopy. This novel TDL system is based on a near-infrared tunable diode laser, whose laser light (emission at 1370 ± 2 nm) is directed via an optical fiber into a second White-type multiple reflection cell, mounted at the inner walls of the AIDA vessel.[24] Data evaluation closely follows the procedure described by Gurlit et al.[25] Both the FISH and the TDL instruments provide a time resolution of about 1 Hz with an overall accuracy of 5−10% including systematic errors. The difference between the FISH total water and TDL interstitial water measurements directly gives the liquid water

mass concentration of the supercooled solution droplets, a quantity needed to infer the composition of the STS aerosols generated in our experiment.

Aerosol Measurements. Size distributions of the aerosol particles were measured with a differential mobility analyzer (DMA), connected to a condensation particle counter (CNC3010, TSI). To avoid evaporation of the supercooled solution droplets during size classification, the DMA was modified for operation inside the isolating housing of the AIDA chamber.[26] Total aerosol sulfate and nitrate mass concentrations of the binary H_2SO_4/H_2O and ternary $H_2SO_4/H_2O/HNO_3$ solution droplets were determined by ion chromatographic analysis of nylon filter samples, type Nylabsorb (Gelman Sciences), which minimize evaporation losses in particular of nitric acid, as described in detail in our recent publication.[8] To minimize adsorptive losses of HNO_3 in the sampling tube, a heated Teflon tube ($T = 293$ K) was used in the sampling line. As the filter holders are located outside the cold housing of the AIDA chamber, nitric acid vapor from particles evaporating in the sampling tube as well as the interstitial HNO_3 vapor in equilibrium with the STS droplets will contribute to the Nylon filter loading. However, at a temperature of 193.6 K, the latter fraction can be neglected compared to the predominantly particle-bound HNO_3 mass concentration. Furthermore, back-up filters were used to correct for breakthrough effects. The relative uncertainty in the sulfuric and nitric acid mass concentration was estimated to be 10% and better.[8]

Uptake Experiment. For the presented experiment, the AIDA chamber was cooled to a temperature of 193.6 ± 0.3 K and filled with particle free synthetic air to a pressure of 180 hPa. The aluminum walls of the aerosol chamber were precoated with a thin ice layer, thus acting as water reservoir during the uptake experiment. A mixing fan was permanently operating at constant speed. Supercooled sulfuric acid aerosol particles, generated outside the AIDA chamber as described by Möhler et al.,[22] were then added to the aerosol vessel and characterized by size distribution measurement, filter analysis, and FTIR extinction spectroscopy. After the analysis of the background aerosol, the reactive trace gases ozone and nitrogen dioxide were successively added to the chamber. Ozone was made in pure oxygen (99.999%, Messer Griesheim) with a silent discharge generator; a mixture of 1000 ppm NO_2 in synthetic air was used as received from Messer Griesheim. As will be explained below, the composition of the H_2SO_4/H_2O background aerosol was about 38 wt % H_2SO_4 with a sulfate mass concentration of about 200 $\mu g/m^3$. To cover an extended range of STS aerosol compositions in our uptake experiment, i.e., ending with nearly pure nitric acid solution droplets containing <5 wt % H_2SO_4, the quantity of added NO_2 had to be adequately chosen, also taking into account wall losses of N_2O_5 and HNO_3. Hence, a total amount of 5.46 mmol NO_2 (5.7 ppm) was injected into the AIDA chamber, corresponding to a nitrate mass concentration of about 4.1 mg/m^3 if all NO_2 molecules were processed to particle-bound nitric acid in course of the experiment. Ozone was added in excess by a factor of 40 (0.22 mol, 235 ppm), thus leading to a rapid depletion of NO_2 within a time scale of about 90 min. The different phases of the uptake experiment are nicely illustrated by the FISH and TDL humidity measurements (Figure 2).

Prior to the injection of the H_2SO_4/H_2O droplets, the total and gas phase water mixing ratios are identical and indicate the water vapor pressure over ice at 193.6 K due to the ice-coated AIDA walls. The addition of the background aerosol leaves the gas phase water concentration unaffected but increases

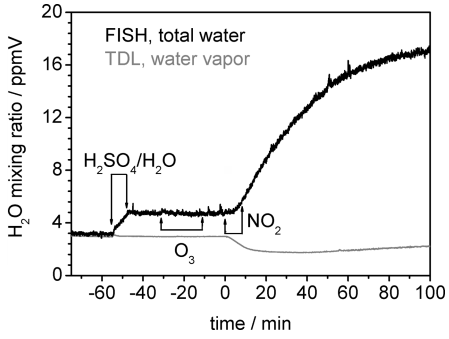

Figure 2. Total water (FISH) and water vapor (TDL) measurements during the N_2O_5 uptake experiment. Time periods of the addition of the H_2SO_4/H_2O aerosol, O_3, and NO_2 are indicated by arrows. Time zero denotes the start of the NO_2 inlet.

the total water mixing ratio by the amount of particle water. Both signals remain constant during the ozone addition but immediately react to the start of the injection of NO_2. The TDL measurement detects the varying water vapor pressure in equilibrium with the particles due to the continuously changing STS aerosol composition, whereas the increase in the total water signal indicates that besides N_2O_5 also H_2O is taken up into the liquid phase. The additional water is transported from the ice covered chamber walls into the aerosol phase. In the next section we will show how the two humidity measurements were used to derive the STS aerosol composition during the uptake experiment.

Determination of Aerosol Composition. The basic requirement for an accurate determination of the continuously varying STS aerosol composition during the N_2O_5 uptake is a precise characterization of the pre-added background aerosol. Various complementary methods were used to derive the composition and mass concentration of the binary H_2SO_4/H_2O solution droplets. First of all, as described in our previous paper,[8] we employed a Mie fitting algorithm to analyze the measured FTIR extinction spectrum using the optical constants of Niedziela et al.[9] as input values. This yields an aerosol composition of 38 wt % H_2SO_4 and a sulfuric acid mass concentration $m(H_2SO_4)$ of 220 $\mu g/m^3$. Consistent with that, the Carslaw et al.[16] thermodynamic model predicts 39 wt % H_2SO_4 as aerosol composition, which gives rise to the measured water vapor pressure in equilibrium with the particles. To further check the retrieved H_2SO_4 mass concentration, we can derive the H_2O mass concentration of the droplets from the difference of the FISH and TDL measurements and calculate the amount of sulfuric acid based on the deduced aerosol composition. This approach leads to $m(H_2SO_4) = 185$ $\mu g/m^3$. In addition, $m(H_2SO_4) = 175$ $\mu g/m^3$ is obtained from the ion chromatographic analysis of a Nylon filter sample. The slight deviation of $m(H_2SO_4)$ retrieved from the FTIR spectrum analysis may be due to the fact that low-temperature optical constants of H_2SO_4/H_2O are only available down to 210 K, but not for the actual AIDA temperature of 193.6 K. Averaging over all results, we adopt 38 ± 1 wt % H_2SO_4 and $m(H_2SO_4) = 195 \pm 20$ $\mu g/m^3$ to characterize the background aerosol.

After the addition of ozone and NO_2, apart from the accompanying FTIR spectra recording, only the two humidity measurements operate at an adequate time resolution to detect the rapid changes in the STS aerosol composition. The time interval needed for sampling filter probes with a sufficient mass loading for the subsequent ion chromatographic analysis, however, is too long, thus providing only some rough average values of the nitric and sulfuric acid mass concentrations during the N_2O_5 uptake. But the technique can be used to determine

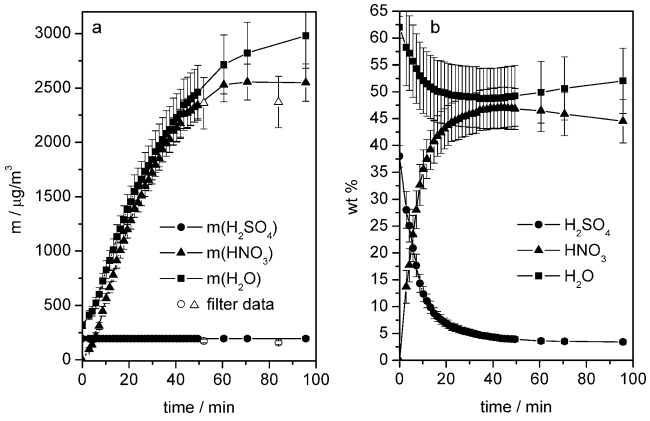

Figure 3. Time evolution of the mass concentration (a) and composition (b) of the supercooled $H_2SO_4/H_2O/HNO_3$ solution droplets during the AIDA uptake experiment, as derived from filter analyses, humidity measurements, and the Carslaw et al.[16] thermodynamic model. Note that the solid lines are only intended as guide to the eye; modeled time profiles of mass concentrations and STS particle compositions are shown in Figure 7.

the final amount of H_2SO_4 and HNO_3 at stationary conditions after the depletion of NO_2. Analyses of filter samples taken 52 and 84 min after the NO_2 addition indicate that, within the given uncertainty range of the method, the sulfuric acid mass concentration remains constant; i.e., no detectable aerosol loss takes place during the time period of the N_2O_5 uptake. Thus, we can employ a constant $m(H_2SO_4) = 195 \pm 20$ $\mu g/m^3$ as sulfuric acid mass concentration throughout the entire uptake experiment. Additionally, the current particle water amount $m(H_2O)$ is obtained at each second from the difference of the FISH and TDL measurements with an estimated accuracy of 10%. The remaining quantity needed to deduce the STS composition, i.e., the particle-bound nitric acid mass concentration $m(HNO_3)$, can be calculated using the measured water vapor pressure in combination with the Carslaw et al.[16] thermodynamic model. By feeding the model with the measured sulfuric acid and total water mass concentration, $m(HNO_3)$ was iteratively adjusted until the measured H_2O vapor pressure was predicted. The uncertainty range of the nitric acid mass concentration was estimated by taking into account a 10% error in the water vapor pressure, thus reflecting the uncertainty range of the TDL measurements and possible inaccuracies in the parametrization of this quantity in the Carslaw et al.[16] model.

Figure 3a finally shows the time evolution of $m(H_2SO_4)$, $m(H_2O)$, and $m(HNO_3)$ during the uptake experiment, as derived from the analysis discussed in this section. The results of the analyses of the two filter probes which where sampled in the final phase of the uptake experiment at near constant $m(HNO_3)$ are shown for comparison. These data closely fit in the $m(HNO_3)$ time profile derived using the TDL water vapor data in combination with the Carslaw et al.[16] thermodynamic model, thus validating our approach to derive the STS aerosol composition. The actual aerosol composition expressed in terms of wt % H_2SO_4, wt % H_2O, and wt % HNO_3 is shown in Figure 3b, documenting the successive conversion of the binary H_2SO_4/H_2O background aerosol into nearly pure nitric acid solution droplets. These directly measured aerosol parameters will then be compared to the values retrieved from the FTIR spectra analysis, whose procedural details are described in the next section.

FTIR Measurements: Trace Gas Mixing Ratios and Retrieval of Aerosol Parameters. FTIR spectra were recorded at time intervals of 90 s during the uptake experiment. In addition to broad-band extinction features of the supercooled solution droplets, they also reveal narrow absorption bands of the reactive trace gases O_3, NO_2, N_2O_4 (in equilibrium with NO_2), and N_2O_5. Prior to the analysis of the STS extinction spectra, these gas absorption features were subtracted using reference spectra obtained from a separate AIDA experiment studying the $O_3 + NO_2$ reaction without pre-added sulfuric acid aerosol particles at 193.6 K. Mixing ratios of O_3 and NO_2 were retrieved using the KOPRA algorithm[13] with the HITRAN 2000[6] spectroscopic parameters as input values. The spectral intervals 2160−2040 cm^{-1} (O_3) and 1680−1540 cm^{-1} (NO_2) were used for the fit. The N_2O_4 concentration was obtained using the temperature-dependent $2NO_2 \rightleftarrows N_2O_4$ equilibrium constant tabulated in the current JPL report (http://jpldataeval.jpl.nasa.gov/). As for N_2O_5, we used the integrated intensity of the absorption band near 1250 cm^{-1} measured by Cantrell et al.[27] to deduce the mixing ratio. The time evolution of the trace gas concentrations will be shown in a later section of this article (Figure 6) when the measured mixing ratios are compared with those calculated with the numerical model based on tabulated kinetic data of the $O_3 + NO_2$ reaction.

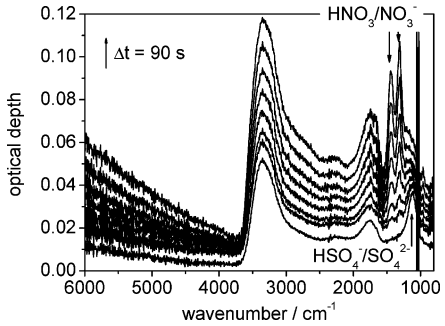

Figure 4. FTIR spectra series documenting the N_2O_5 hydrolysis into the supercooled sulfuric acid solution droplets. The bottom spectrum was recorded before the NO_2 inlet; subsequent spectra (from bottom to top) were monitored in time steps of 90 s after the NO_2 addition.

Figure 4 shows the sequence of FTIR extinction spectra recorded after the addition of O_3 and NO_2 with all trace gas absorption features subtracted. The subtraction procedure failed in the spectral region between 1080 and 1010 cm^{-1} due to saturation effects as a result of the high ozone concentration. The spectra series clearly demonstrates the successive buildup of nitric acid in the supercooled solution droplets, as can be seen by the continuous increase of the intensity of the characteristic doublet feature at about 1310 and 1450 cm^{-1} with contributions from the ν_3 mode of the nitrate ion centered at 1350 cm^{-1}, appearing as doublet in the spectra, and ν_3 and ν_4 of nitric acid at 1304 and 1429 cm^{-1}.[28]

To derive the STS composition and mass concentration, spectra calculated from Mie theory were fitted to the measured FTIR extinction spectra, assuming log-normally distributed particle sizes. The imaginary refractive indices k of the STS droplets with wts = wt % H_2SO_4 and wtn = wt % HNO_3 were calculated using the Biermann et al.[11] mixing rule (eq 1) with the Niedziela et al.[9] H_2SO_4/H_2O (k_s) as well as the Norman et al.[10] HNO_3/H_2O (k_n) binary data sets as input values.

$$k(\lambda,T,\mathrm{wts},\mathrm{wtn}) = \frac{\mathrm{wts}}{\mathrm{wts}+\mathrm{wtn}}\,k_s(\lambda,T,\mathrm{wts}+\mathrm{wtn}) + \frac{\mathrm{wtn}}{\mathrm{wts}+\mathrm{wtn}}\,k_n(\lambda,T,\mathrm{wts}+\mathrm{wtn}) \quad (1)$$

Note that k_s and k_n data corresponding to an acid weight percentage of wts + wtn have to be employed in the mixing

rule approach, i.e., implying similar water activities for ternary solutions with weight percentages wt(total) = wts + wtn and binary solutions with wt(total) = wts or wt(total) = wtn. A subtractive Kramers−Kronig (SKK) expression[29] was used to calculate the corresponding real refractive indices *n*. Here, we closely followed the guideline presented by Norman et al.[15] to correct for truncation errors in the Kramers−Kronig transform. So the wavenumber range of the *k* data was extended to 400 cm^{-1} using the room-temperature data sets of Palmer and Williams[30] for H_2SO_4/H_2O and Querry and Tyler[28] for HNO_3/H_2O. The expansion point in the SKK integration was set to 5000 cm^{-1}, the corresponding value for the real refractive index was obtained from the model of Luo et al.,[31] using the FORTRAN routine provided by Krieger et al.[32] STS composition and mass concentration were simultaneously retrieved by minimizing the summed squared residuals between measured and calculated extinction spectra, using wts and wtn as well as the parameters of the aerosol size distribution (i.e., N = aerosol number density, σ_g = mode width, and CMD = count median diameter) as fitting parameters. The downhill simplex method was used as the optimization technique.[33] Total aerosol volume densities were then calculated from the retrieved size distribution parameters and converted into STS mass concentrations using an analytical expression for the densities of the ternary solutions.[32]

Modeling the N_2O_5 Uptake. Regarding the gas phase chemistry, the oxidation of NO_2 by O_3 (R1) as well as the simultaneous dimerization/decomposition reactions (R2, R-2) and (R3, R-3) have to be considered.

$$NO_2 + O_3 \rightarrow NO_3 + O_2 \qquad \text{(R1)}$$

$$2NO_2 + M \rightleftarrows N_2O_4 + M \qquad \text{(R2, R-2)}$$

$$NO_2 + NO_3 + M \rightleftarrows N_2O_5 + M \qquad \text{(R3, R-3)}$$

Additional NO_3 reactions as well as the homogeneous hydrolysis of N_2O_5 proved to be negligible due to the low temperature encountered in our experiment. The rate constant for reaction R1 is calculated following the most recent IUPAC recommendation (http://www.iupac-kinetic.ch.cam.ac.uk). However, experimental backup for this parametrization was missing so far for temperatures below 230 K. The equilibrium constants for the formation and dissociation of N_2O_4 and N_2O_5 are taken from the current JPL tabulation, where the range of validity is stated as 200 K < T < 300 K. Our experiment thus provides a first test whether the tabulated temperature dependencies of the rate and equilibrium constants under consideration may be extrapolated to temperatures as low as 193.6 K, an interesting point regarding the modeling of stratospheric processes.

Similar to our earlier work,[34,35] the transport rate of N_2O_5 molecules to the particle surface is calculated using the transition regime correction proposed by Dahneke,[36]

$$J = 4\pi R D_g \beta (c_\infty - c_s) \qquad (2)$$

with

$$\beta = \frac{Kn_D + 1}{\frac{2Kn_D(Kn_D + 1)}{\gamma} + 1} \qquad Kn_D = \frac{2D_g}{\upsilon_g R} \qquad (3)$$

where R denotes the radius of the particles, D_g is the N_2O_5 gas phase diffusion coefficient, and c_∞ and c_s are the gas phase bulk and surface concentrations, respectively. γ represents the effective reaction probability and υ_g is the average thermal velocity. Please note that Dahneke's formalism differs from the simple resistance approach often employed in the literature. The partitioning of water and HNO_3 formed by the heterogeneous hydrolysis of N_2O_5 between gas and particle phase is assumed to establish instantaneously following the parametrization developed by Carslaw et al.[37] The losses of gaseous N_2O_5 and HNO_3 to the chamber walls are treated as irreversible first-order reactions:

$$N_2O_5 \rightarrow \text{products} \qquad \text{(R4)}$$

$$HNO_3 \rightarrow \text{products} \qquad \text{(R5)}$$

The rate constants for R4 and R5 as well as γ are adjusted for optimum agreement between experimental and model results. However, because R4 and R5 are completely controlled by diffusion their rates are linked via the values of the respective diffusion coefficients. The wall induced depletion of NO_2, NO_3, O_3, and particulate matter turned out to be negligible under the conditions of our experiment. Starting from a log-normal fit to the measured initial size distribution of the sulfuric acid aerosol, the FACSIMILE code (Computer software for modeling processes and chemical reactions, MCPA-Software Ltd, http://www.mcpa-software.com/facsimileframe.html) is used to compute the time evolution of the trace gas concentrations as well as the mass and composition of the particulate phase. Due to the rapid uptake of water by the aerosol droplets during the early stages of the experiment the water vapor pressure dropped well below its saturation value (see Figure 2), because the transport of water from the ice covered walls is too slow to maintain equilibrium. Therefore, the time evolution of the water gas phase concentration measured by TDL spectroscopy is used directly within the numerical simulation.

Results and Discussion

Quantitative Test of the Mixing Rule Approach. Figure 5 shows a compilation of six selected FTIR extinction spectra of the ternary $H_2SO_4/H_2O/HNO_3$ solution droplets recorded during the uptake experiment. Measured STS compositions range from 28 wt % H_2SO_4 + 14 wt % HNO_3 (panel a) to 6 wt % H_2SO_4 + 45 wt % HNO_3 (panel f). The measured spectra are compared with the best fit results from the Mie calculations using the optical constants obtained from the mixing rule approach. STS compositions and mass concentrations retrieved from the analysis of the FTIR spectra are summarized in Table 1, the independently measured aerosol parameters are shown as comparison.

The first remarkable aspect is the overall nice agreement between measured and calculated spectra. This clearly justifies the approach of calculating the ternary $H_2SO_4/H_2O/HNO_3$ *k* spectra as linear superposition of the two binary H_2SO_4/H_2O and HNO_3/H_2O *k* data sets, which relies on the assumption that no solvent induced band shifts or even additional absorption features become visible in the ternary mixture, e.g., caused by strong intermolecular interactions or a chemical reaction between the individual species. The subtle deviations of the Mie calculations from the measured FTIR extinction spectra, which can be made out in the spectra collection shown in Figure 5, were already observed in our previous study,[8] i.e., may be traced back to slight inaccuracies of the employed binary data sets of optical constants. So, the extinction band of undissociated HNO_3 at 1672 cm^{-1} is barely visible in the measured spectra but contrarily overestimated in the Mie calculations of the STS

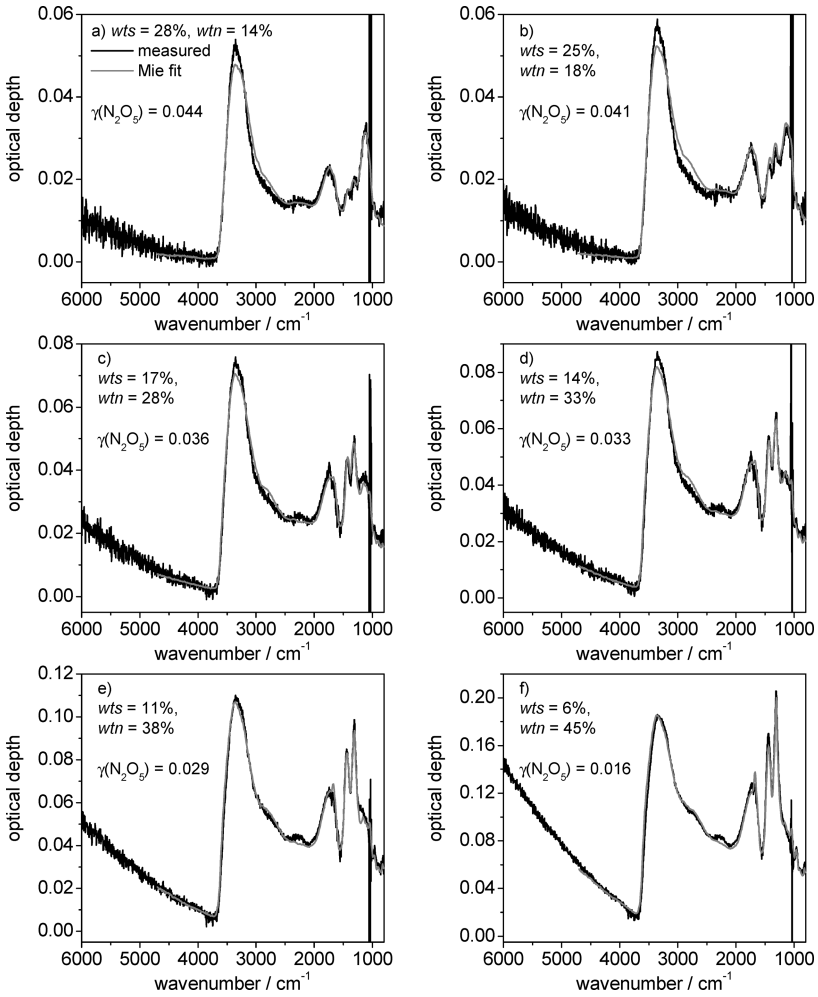

Figure 5. FTIR extinction spectra of supercooled $H_2SO_4/H_2O/HNO_3$ droplets obtained in this work (black lines) and best fit results based on Mie calculations using the mixing rule approach (gray lines). Mie fits only cover the 4700−800 cm^{-1} range, the wavenumber regime for which the H_2SO_4/H_2O and HNO_3/H_2O data sets of optical constants are tabulated. Measured STS compositions are indicated in each panel, together with corresponding values of the uptake coefficient $\gamma(N_2O_5)$, as derived from the model calculations whose results will be described in detail in the next section. Retrieved STS compositions and mass concentrations are summarized in Table 1.

spectra with high wt % HNO_3. This could be explained by a temperature effect because the binary HNO_3/H_2O optical constants were only obtained at a temperature of 220 K. Cooling from 220 K down to the actual AIDA temperature of 193.6 K may further promote the dissociation of HNO_3 into nitrate and hydronium ions, thus explaining this spectral discrepancy. Furthermore, especially in case studies a and b, there are spectral differences in the wavenumber range from 3600 to 2500 cm^{-1}, covering the extinction features of H_2O and H_3O^+, where the calculated extinction band centered at about 3300 cm^{-1} is somewhat broadened as compared to the measured spectra. We believe that this may be a result of a slightly poorer performance of the Norman et al.[10] HNO_3/H_2O refractive index data sets in this wavenumber regime, as already discussed in our previous work.[8] Particularly, the binary *k* index data sets for 35 wt % HNO_3 and 45 wt % HNO_3 of Norman et al.[10] show this broadened 3300 cm^{-1} absorption band in comparison with the corresponding Biermann et al.[11] *k* data sets (see Figures 1 and 9 in our preceding paper[8]), presumably reflecting an improperly subtracted scattering contribution in the aerosol spectra which were used to extract the refractive index data sets. Exactly an interpolation between these discrete measurements for 35 and 45 wt % HNO_3 had to be employed to calculate the nitric acid absorption contribution to the ternary $H_2SO_4/H_2O/HNO_3$ system in our case studies a and b, having a total acid concentration wts + wtn of 42−43 wt %. Thus, the subtle spectral mismatch already introduced into the binary HNO_3/H_2O system simply propagates into the extinction spectra of the ternary solution droplets.

In addition to the good accordance between measured and calculated infrared extinction spectra of the STS droplets, also the measured aerosol parameters (composition and mass concentration) are precisely matched by those retrieved from the analysis of the FTIR spectra (Table 1). In most cases, the retrieved wt % H_2SO_4 and wt % HNO_3 as well as the total STS mass concentration are only slightly overestimated. Thus, we can clearly recommend the implementation of the mixing rule approach in the retrieval algorithms to quantitatively analyze the FTIR spectra of STS droplets in terms of aerosol composition and mass concentration, with a precision as indicated by the uncertainty ranges quoted in Table 1. The small, apparently systematic deviations between measured and retrieved aerosol parameters may be a result of a deficiency of the simple Biermann et al.[11] mixing rule, an argument already brought forward by Norman et al.[15] to explain the small spectral differences between their directly derived STS refractive index data sets and those calculated by means of the mixing rule. Unfortunately, none of the six discrete refractive index data sets for STS aerosols derived by Norman et al.[15] exactly matched the STS aerosol compositions evolving in our uptake experi-

TABLE 1: Comparison of STS Compositions (wt % H_2SO_4, wt % HNO_3) and Mass Concentrations ($m_{STS} = m(H_2SO_4) + m(HNO_3) + m(H_2O)$) Retrieved from the Analysis of the FTIR Extinction Spectra with Those Simultaneously Derived from Filter Sampling, Humidity Measurements, and the Carslaw Thermodynamic Model[16]

	wt % H_2SO_4	wt % HNO_3	m_{STS} (mg/m^3)
	a, $\gamma(N_2O_5) = 0.044$:		
fit result	32 ± 2	10 ± 2	0.73 ± 0.03
measured	28 ± 3	14 ± 3	0.70 ± 0.05
	b, $\gamma(N_2O_5) = 0.041$:		
fit result	28 ± 2	18 ± 2	0.87 ± 0.03
measured	25 ± 2	18 ± 3	0.78 ± 0.05
	c, $\gamma(N_2O_5) = 0.036$:		
fit result	17 ± 2	31 ± 2	1.22 ± 0.04
measured	17 ± 2	28 ± 3	1.11 ± 0.07
	d, $\gamma(N_2O_5) = 0.033$:		
fit result	17 ± 2	34 ± 2	1.5 ± 0.1
measured	14 ± 2	33 ± 4	1.4 ± 0.1
	e, $\gamma(N_2O_5) = 0.029$:		
fit result	12 ± 2	41 ± 2	2.0 ± 0.1
measured	11 ± 1	38 ± 4	1.8 ± 0.1
	f, $\gamma(N_2O_5) = 0.016$:		
fit result	9 ± 2	48 ± 2	3.8 ± 0.1
measured	6 ± 1	45 ± 4	3.2 ± 0.2

[a] A constant ±2 wt % error was assumed for the FTIR retrieval results due to the uncertainty range of the employed optical constants.[9,10] Also indicated is the value of the uptake coefficient $\gamma(N_2O_5)$ for the different STS compositions, as derived from the model calculations whose results will be described in detail in the next section.

ment. Hence, we cannot examine whether these directly measured data sets would further improve the already good quality of our fit results. Biermann et al.[11] proposed their mixing rule on the assumption that the ionic strength and water activity are the key parameters influencing the absorption features of the components in the ternary $H_2SO_4/H_2O/HNO_3$ mixture. As the water activity is nearly constant for a given wts + wtn, meaning, e.g., that the water activities for binary 40 wt % sulfuric or nitric acid solutions as well as ternary 10 wt % H_2SO_4 + 30 wt % HNO_3 or 30 wt % H_2SO_4 + 10 wt % HNO_3 are almost identical, the mixing rule was formulated as shown in eq 1. To further improve the accuracy of the mixing rule, the exact ionic speciation in the ternary STS droplets has to be known, which primarily determines the spectral shape of the infrared absorption bands. Thus, to accurately describe the H_2SO_4 contribution to the infrared absorption spectrum of a ternary 10 wt % H_2SO_4 + 30 wt % HNO_3 solution, one should employ the absorption spectrum of the binary sulfuric acid solution in the mixing rule calculation, which shows the identical ionic speciation, i.e., the same relative amount of the sulfate and bisulfate ions, as in the ternary solution. For the same reason, the binary HNO_3/H_2O absorption spectrum employed in eq 1 should exhibit the same degree of dissociation of molecular nitric acid into nitrate ions as in the ternary 10 wt % H_2SO_4 + 30 wt % HNO_3 solution. Unfortunately, experimental data about the dissociation behavior of sulfuric and nitric acid in ternary solutions, required to test this modified mixing rule approach, are scarce. The recent Raman spectroscopic study by Minogue et al.[38] provides first insight into the ionic and molecular speciation in ternary $H_2SO_4/H_2O/HNO_3$ mixtures. The quantitative analysis, however, was hindered due to band overlap, thus revealing only semiquantitative results concerning the concentration and temperature dependence of the ionic speciation in the ternary system. Generally, it should be noted that when subtle modifications of the original Biermann et al.[11] mixing rule approach, deduced from a comparison between

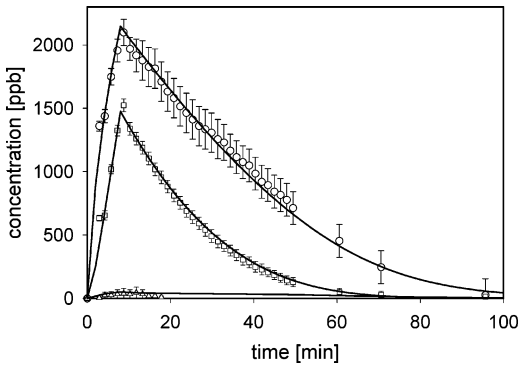

Figure 6. Time evolution of trace gas mixing ratios: circles, NO_2; squares, N_2O_4; triangles, N_2O_5. The simulation results are represented by solid lines.

directly measured STS extinction spectra and those calculated by superposition of binary sulfuric and nitric acid droplet spectra, are discussed, the aerosol composition of both the binary and the ternary systems has to be known with high accuracy. For example, Niedziela et al.[9] and Norman et al.[10,15] report an uncertainty in composition of approximately ±2 wt % for H_2SO_4 and HNO_3 in their ternary and binary refractive index data sets. Thus, the combined uncertainties in the composition of the binary and ternary aerosol spectra may also contribute to the spectral differences observed between their directly measured STS refractive index data sets and those calculated by means of the mixing rule approach. In this context, new measurements of STS refractive index data sets by Myhre et al.,[39] obtained from specular reflectance spectra of ternary $H_2SO_4/H_2O/HNO_3$ solutions with precisely known composition, might provide a more stringent test of the Biermann et al.[11] mixing rule.

Uptake Coefficient $\gamma(N_2O_5)$ on Liquid Sulfuric Acid and STS Droplets. Having convinced ourselves that the composition of the ternary solution droplets could be accurately retrieved from their FTIR spectra, we now proceed to analyze the overall multiple kinetics of the uptake experiment. Starting the model run with an injection of 5.46 mmol of NO_2 results in a slight underestimation of the initial NO_2 and N_2O_4 concentrations compared to the FTIR data. Optimum consistency between experiment and simulation is achieved by increasing the amount of injected NO_2 by 3.8%. The time evolution of the trace gas concentrations calculated this way is compared to the measured one in Figure 6. The good agreement observed for both NO_2 and N_2O_4 suggests that the recommended parametrization for the temperature dependence of the rate constant for reaction R1 remains reliable down to 193.6 K. The same applies to the equilibrium constant of reactions R2/R-2, because a significantly incorrect value would inevitably deteriorate the numerically predicted NO_2 mixing ratio.

As soon as NO_3 becomes available, N_2O_5 is rapidly produced via reaction R3. On the other hand, the dissociation R-3 proceeds very slowly at temperatures as low as 193.6 K. The dominant sinks for N_2O_5 are the uptake into the particles followed by hydrolysis to HNO_3 and the irreversible loss to the chamber walls. Due to these efficient depletion processes, the N_2O_5 mixing ratio never exceeded a value of about 40 ppb. Unfortunately, this low concentration is close to the detection limit of our FTIR analysis, leading to a large uncertainty of about a factor of 2. Because of these reasons, our experiment was not sensitive enough to allow for an unambiguous consistency check of the JPL equilibrium constant recommendation for the reaction pair R3/R-3.

Figure 7 compares the measured and modeled time profiles of mass concentrations and STS particle compositions. The

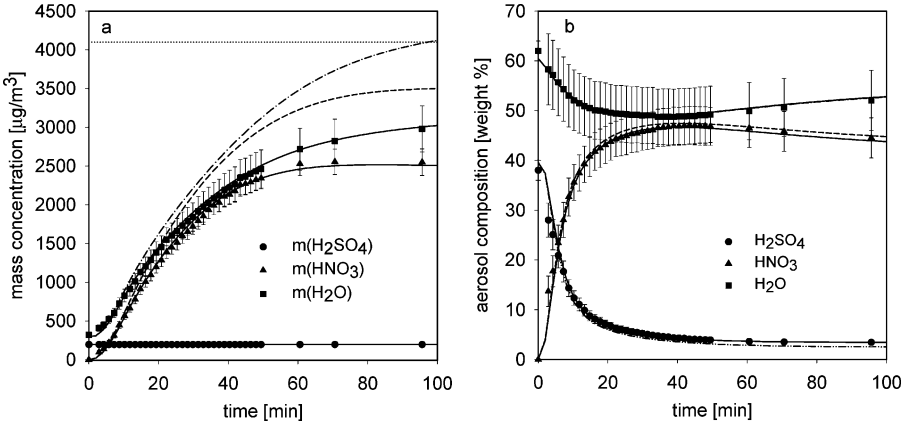

Figure 7. Measured and modeled time evolution of mass concentration of aerosol compounds (a) and particle composition (b). The experimental data correspond to Figure 3 (squares, H_2O; triangles, HNO_3; circles, H_2SO_4). The simulation results for constant effective reaction probability γ are represented by broken lines (-•-, H_2O; - - -, HNO_3; -••-, H_2SO_4). The solid lines are calculated assuming γ to decrease exponentially with time. The dotted line in panel a shows the maximum HNO_3 mass concentration if all injected NO_2 molecules were processed to particle-bound nitric acid.

initial value for the effective N_2O_5 reaction probability γ on pure sulfuric acid droplets is determined to be 0.05, consistent with the results cited in the latest IUPAC compilation. However, because the uptake rate of N_2O_5 into the particles is controlled by γ and the wall loss reaction R4, the uncertainty of the measured N_2O_5 gas phase mixing ratio propagates into the values fitted for γ and for the rate constant of R4. Nevertheless, Figure 7a clearly demonstrates that the simulation based on the supposition of γ remaining constant over all phases of the experiment (broken lines) badly fails to reproduce the measured time evolution of the aerosol mass concentrations of HNO_3 and H_2O. On the other hand, very good agreement between experimental and modeling results is achieved assuming γ to decrease exponentially with time (solid lines), i.e., $\gamma = 0.05 \exp(-7.8 \times 10^{-4}\ s^{-1} \times t)$. Exemplary values of γ for different STS compositions, i.e., corresponding to different times during the uptake experiment, are given in Table 1. Figure 7b reveals that the relative aerosol composition is rather insensitive to the diminishing of γ because an overestimated formation of HNO_3 is more or less compensated for by an increased uptake of H_2O. Because the wall loss of N_2O_5 is diffusion controlled and the speed of the mixing fan was kept constant, it appears unreasonable to consider an increasing rate of R4 to explain the suppression of aerosol nitrate formation. We therefore conclude that due to the increasing concentration of nitrate in the particles formed by the hydrolysis of N_2O_5 the effective reaction probability γ decays with a lifetime (1/e time) of about 21 min under the conditions of our experiment, which exactly corresponds to the time when the changes in the STS composition are leveling off (Figure 7b). This finding is not significantly affected by the uncertainty of the initial value for γ. Therefore, our study provides additional strong evidence that the nitrate effect well documented in room temperature experiments is still operative down to 193.6 K. Preliminary tests seem to indicate that the low temperature nitrate effect can be alternatively modeled in a quantitative manner employing a direct functional dependence of γ on the concentrations of HNO_3 and H_2O, similar in spirit to the formalism proposed by Mentel et al.[17] and by Hallquist et al.[40] However, additional experiments will be necessary to support this approach.

Conclusions

On the basis of a series of mid-infrared extinction spectra of supercooled $H_2SO_4/H_2O/HNO_3$ solution (STS) droplets, obtained from a simulation experiment at the low-temperature aerosol chamber facility AIDA, we have tested the performance of a mixing rule approach for the quantitative analysis of the infrared spectra in terms of aerosol composition and mass concentration. As a result of our experimental strategy to generate the ternary solution droplets, i.e., uptake of N_2O_5 (from the $O_3 + NO_2$ reaction) into pre-added sulfuric acid droplets at 193.6 K, the analysis spanned a broad range of different STS compositions, starting with binary H_2SO_4/H_2O droplets and ending with nearly pure HNO_3/H_2O aerosol particles. The aerosol parameters retrieved from the FTIR spectra were directly compared to those simultaneously measured with the comprehensive diagnostic tools of the AIDA chamber. Keeping in mind the results from a previous study,[8] which demonstrated the good performance of the refractive index data sets from Niedziela et al.[9] and Norman et al.[10] in reproducing infrared extinction spectra of binary H_2SO_4/H_2O and HNO_3/H_2O solution droplets, we used these data sets to calculate the optical constants of the ternary solution droplets with the mixing rule proposed by Biermann et al.[11] We observed good agreement between measured and calculated STS extinction spectra. Minor spectral discrepancies may be a result of (i) slight inaccuracies of the employed binary data sets, (ii) a temperature effect, as the binary optical constants are not available for a temperature as low as 193.6 K, or (iii) the simplicity of the mixing rule, relying on the additivity of the two binary *k* spectra in the ternary mixture. Measured STS compositions and mass concentrations during the uptake experiment were nicely matched by the FTIR retrieval results. The percentage error in the retrieved aerosol mass concentration never exceeded 20%, being in most cases even as low as 10%. Maximum deviations between measured and retrieved aerosol compositions (wt % H_2SO_4 and wt % HNO_3) were in the order of 3−4 wt %.

In addition to the spectroscopic results, the uptake experiment proved to be suitable to clarify the magnitude of the nitrate effect in the uptake of N_2O_5 on STS aerosols. A numerical model, including all important nitrogen oxide gas phase reactions, chamber specific wall loss rates of N_2O_5 and HNO_3, as well as the heterogeneous conversion of N_2O_5 into particle-bound nitric acid, was employed to calculate the time profiles of trace gas mixing ratios as well as STS mass concentration and composition during the uptake experiment. Here, the uptake coefficient γ was used as adjustable parameter to best fit the experimental data. Measured NO_2 and N_2O_4 time profiles were nicely matched by the model runs, illustrating that the parametrizations employed for the temperature dependence of the required kinetic

data are still precise even when extrapolating to a temperature as low as 193.6 K. Experimental STS mass concentrations could only be accurately mimicked in model runs with γ exponentially decreasing in time, i.e., with increasing nitrate concentration in the particles. From an initial value of $\gamma = 0.05$ for pure H_2SO_4/H_2O solution droplets, γ dropped well below 0.02 when exceeding a nitrate mass fraction of about 40 wt % in course of the uptake experiment, being in good agreement with earlier results from Zhang et al.[20] This shows that the nitrate effect already observed at room temperature is also important under stratospheric conditions and should be accounted for in stratospheric chemistry models.

Acknowledgment. We are grateful for the continuous support by all members of the AIDA staff. We thank Elisabeth Kranz for the ion chromatographic analyses of the filter samples and C. E. L. Myhre for helpful discussions about the refractive indices of STS aerosols. We acknowledge the skillful assistance of Volker Ebert and Carsten Giesemann in the analysis of the TDL data. The present work has been funded by BMBF (AFO2000 Project POSTA, 07ATF04).

References and Notes

(1) Beyerle, G.; Luo, B. P.; Neuber, R.; Peter, T.; McDermid, I. S. *J. Geophys. Res. (Atmos.)* **1997**, *102*, 3603.

(2) Schreiner, J.; Voigt, C.; Weisser, C.; Kohlmann, A.; Mauersberger, K.; Deshler, T.; Kröger, C.; Rosen, J.; Kjome, N.; Larsen, N.; Adriani, A.; Cairo, F.; Di Donfrancesco, G.; Ovarlez, J.; Ovarlez, H.; Dörnbrack, A. *J. Geophys. Res. (Atmos.)* **2003**, *108* (D5), 8313.

(3) Schreiner, J.; Voigt, C.; Zink, P.; Kohlmann, A.; Knopf, D.; Weisser, C.; Budz, P.; Mauersberger, K. *Rev. Sci. Instrum.* **2002**, *73*, 446.

(4) Zasetsky, A. Y.; Sloan, J. J.; Escribano, R.; Fernandez, D. *Geophys. Res. Lett.* **2002**, *29*, 2071.

(5) Zasetsky, A. Y.; Khalizov, A. F.; Sloan, J. J. *Appl. Opt.* **2004**, *43*, 5503.

(6) Rothman, L. S.; Barbe, A.; Benner, D. C.; Brown, L. R.; Camy-Peyret, C.; Carleer, M. R.; Chance, K.; Clerbaux, C.; Dana, V.; Devi, V. M.; Fayt, A.; Flaud, J. M.; Gamache, R. R.; Goldman, A.; Jacquemart, D.; Jucks, K. W.; Lafferty, W. J.; Mandin, J. Y.; Massie, S. T.; Nemtchinov, V.; Newnham, D. A.; Perrin, A.; Rinsland, C. P.; Schroeder, J.; Smith, K. M.; Smith, M. A. H.; Tang, K.; Toth, R. A.; Vander Auwera, J.; Varanasi, P.; Yoshino, K. *J. Quant. Spectrosc. Radiat. Transfer* **2003**, *82*, 5.

(7) Massie, S. T.; Goldman, A. *J. Quant. Spectrosc. Radiat. Transfer* **2003**, *82*, 413.

(8) Wagner, R.; Mangold, A.; Möhler, O.; Saathoff, H.; Schnaiter, M.; Schurath, U. *Atmos. Chem. Phys.* **2003**, *3*, 1147.

(9) Niedziela, R. F.; Norman, M. L.; DeForest, C. L.; Miller, R. E.; Worsnop, D. R. *J. Phys. Chem. A* **1999**, *103*, 8030.

(10) Norman, M. L.; Qian, J.; Miller, R. E.; Worsnop, D. R. *J. Geophys. Res. (Atmos.)* **1999**, *104*, 30571.

(11) Biermann, U. M.; Luo, B. P.; Peter, T. *J. Phys. Chem. A* **2000**, *104*, 783.

(12) Eldering, A.; Irion, F. W.; Chang, A. Y.; Gunson, M. R.; Mills, F. P.; Steele, H. M. *Appl. Opt.* **2001**, *40*, 3082.

(13) Höpfner, M. *J. Quant. Spectrosc. Radiat. Transfer* **2004**, *83*, 93.

(14) McPheat, R. A.; Bass, S. F.; Newnham, D. A.; Ballard, J.; Remedios, J. J. *J. Geophys. Res. (Atmos.)* **2002**, *107*, 4371.

(15) Norman, M. L.; Miller, R. E.; Worsnop, D. R. *J. Phys. Chem. A* **2002**, *106*, 6075.

(16) Carslaw, K. S.; Clegg, S. L.; Brimblecombe, P. *J. Phys. Chem.* **1995**, *99*, 11557.

(17) Mentel, T. F.; Sohn, M.; Wahner, A. *Phys. Chem. Chem. Phys.* **1999**, *1*, 5451.

(18) Mozurkewich, M.; Calvert, J. G. *J. Geophys. Res. (Atmos.)* **1988**, *93*, 15889.

(19) Hanson, D. R. *Geophys. Res. Lett.* **1997**, *24*, 1087.

(20) Zhang, R. Y.; Leu, M. T.; Keyser, L. F. *Geophys. Res. Lett.* **1995**, *22*, 1493.

(21) Möhler, O.; Büttner, S.; Linke, C.; Schnaiter, M.; Saathoff, H.; Stetzer, O.; Wagner, R.; Krämer, M.; Mangold, A.; Ebert, V.; Schurath, U. *J. Geophys. Res.* **2005**, *110*, D11210.

(22) Möhler, O.; Stetzer, O.; Schaefers, S.; Linke, C.; Schnaiter, M.; Tiede, R.; Saathoff, H.; Krämer, M.; Mangold, A.; Budz, P.; Zink, P.; Schreiner, J.; Mauersberger, K.; Haag, W.; Kärcher, B.; Schurath, U. *Atmos. Chem. Phys.* **2003**, *3*, 211.

(23) Zöger, M.; Afchine, A.; Eicke, N.; Gerhards, M. T.; Klein, E.; McKenna, D. S.; Mörschel, U.; Schmidt, U.; Tan, V.; Tuitjer, F.; Woyke, T.; Schiller, C. *J. Geophys. Res. (Atmos.)* **1999**, *104*, 1807.

(24) Ebert, V.; Teichert, H.; Giesemann, C.; Saathoff, H.; Schurath, U. *Technisches Messen* **2005**, *72*, 23.

(25) Gurlit, W.; Zimmermann, R.; Giesemann, C.; Fernholz, T.; Ebert, V.; Wolfrum, J.; Platt, U.; Burrows, J. P. *Appl. Opt.* **2005**, *44*, 91.

(26) Seifert, M.; Tiede, R.; Schnaiter, M.; Linke, C.; Möhler, O.; Schurath, U.; Ström, J. *J. Aerosol Sci.* **2004**, *35*, 981.

(27) Cantrell, C. A.; Davidson, J. A.; McDaniel, A. H.; Shetter, R. E.; Calvert, J. G. *Chem. Phys. Lett.* **1988**, *148*, 358.

(28) Querry, M. R.; Tyler, I. L. *J. Chem. Phys.* **1980**, *72*, 2495.

(29) Ahrenkiel, R. K. *J. Opt. Soc. Am.* **1971**, *61*, 1651.

(30) Palmer, K. F.; Williams, D. *Appl. Opt.* **1975**, *14*, 208.

(31) Luo, B.; Krieger, U. K.; Peter, T. *Geophys. Res. Lett.* **1996**, *23*, 3707.

(32) Krieger, U. K.; Mössinger, J. C.; Luo, B. P.; Weers, U.; Peter, T. *Appl. Opt.* **2000**, *39*, 3691.

(33) Press, W. H.; Teukolsky, S. A.; Vetterling, W. T.; Flannery, B. P. *Numerical Recipes in C: The Art of Scientific Computing*; Cambridge University Press: Cambridge, U.K., 1992.

(34) Kamm, S.; Möhler, O.; Naumann, K. H.; Saathoff, H.; Schurath, U. *Atmos. Environ.* **1999**, *33*, 4651.

(35) Saathoff, H.; Naumann, K. H.; Riemer, N.; Kamm, S.; Möhler, O.; Schurath, U.; Vogel, H.; Vogel, B. *Geophys. Res. Lett.* **2001**, *28*, 1957.

(36) Dahneke, B. *Theory of dispersed multiphase flow*; Academic Press: London, 1983.

(37) Carslaw, K. S.; Luo, B. P.; Peter, T. *Geophys. Res. Lett.* **1995**, *22*, 1877.

(38) Minogue, N.; Riordan, E.; Sodeau, J. R. *J. Phys. Chem. A* **2003**, *107*, 4436.

(39) Myhre, C. E. L.; Grothe, H.; Gola, A. A.; Nielsen, C. J., Optical constants of HNO_3/H_2O and $H_2SO_4/HNO_3/H_2O$ at low temperatures in the infrared region. *J. Phys. Chem. A*, doi: 10.1021/jp0508406.

(40) Hallquist, M.; Stewart, D. J.; Stephenson, S. K.; Cox, R. A. *Phys. Chem. Chem. Phys.* **2003**, *5*, 3453.